© 2017. Published by The Company of Biologists Ltd | Development (2017) 144, 3521-3532 doi:10.1242/dev.149724

RESEARCH ARTICLE

Adenohypophysis placodal precursors exhibit distinctive features within the rostral preplacodal ectoderm

Luisa Sanchez-Arrones[1,2], África Sandonís[1,2], Marcos Julián Cardozo[1,2] and Paola Bovolenta[1,2,*]

ABSTRACT

Placodes are discrete thickenings of the vertebrate cranial ectoderm that generate morpho-functionally distinct structures, such as the adenohypophysis, olfactory epithelium and lens. All placodes arise from a horseshoe-shaped preplacodal ectoderm in which the precursors of individual placodes are intermingled. However, fate-map studies indicated that cells positioned at the preplacodal midline give rise to only the adenohypophyseal placode, suggesting a unique organization of these precursors within the preplacode. To test this possibility, we combined embryological and molecular approaches in chick embryos to show that, at gastrula stage, adenohypophyseal precursors are clustered in the median preplacodal ectoderm, largely segregated from those of the adjacent olfactory placode. Median precursors are elongated, densely packed and, at neurula stage, express a molecular signature that distinguishes them from the remaining preplacodal cells. Olfactory placode precursors and midline neural cells can replace ablated adenohypophyseal precursors up to head-fold stage, although with a more plastic organization. We thus propose that adenohypophyseal placode precursors are unique within the preplacodal ectoderm possibly because they originate the only single placode and the only one with an endocrine character.

KEY WORDS: Adhesion, Cell movement, Midline, Pituitary, Chick, RNA-seq, *Sp8*

INTRODUCTION

Placodes are discrete thickenings of the cranial ectoderm localized in the proximity of the developing vertebrate neural tube. Following a rostral to caudal direction, their derivatives include the anterior region of the pituitary gland, known as the adenohypophysis; the olfactory epithelium; the lens; the inner ear and statoacoustic ganglion; and neurons of the trigeminal, geniculate, petrosal and nodose ganglia (Graham and Shimeld, 2013; McCabe and Bronner-Fraser, 2009). Despite their final morpho-functional diversity, placodes arise from a common horseshoe-shaped domain, known as the preplacodal ectoderm (PPE), that surrounds the neural plate (Schlosser, 2014; Streit, 2004). The PPE is established concomitantly with the sharpening of the border between the non-neural and neural ectoderm at late gastrula stages (Bailey and Streit, 2006; Baker and Bronner-Fraser, 2001; Couly and Le Douarin, 1988; Schlosser, 2006; Streit, 2004) and soon becomes subdivided in two territories. The most caudal will generate the otic and epibranchial placode, whereas the rostral one, abutting the anterior neural folds, generates the adenohypophyseal (AHP), olfactory (OP) and lens (LP) placodes (Cajal et al., 2012; Cobos et al., 2001; Dutta et al., 2005; Eagleson et al., 1995).

As it forms, the PPE acquires the expression of a distinctive combination of transcription factors (TFs) that are thought to confer a common ground state to all placodal progenitors (Bailey et al., 2006; Moody and LaMantia, 2015; Saint-Jeannet and Moody, 2014). These include members of the Six, Eya and Dlx families (Esteve and Bovolenta, 1999; Kobayashi et al., 2000; Saint-Jeannet and Moody, 2014; Sato et al., 2010; Schlosser and Ahrens, 2004; Streit, 2007), over which others are added to specify rostral or caudal identities (Schlosser and Ahrens, 2004). The TF *Pax6* is among those that define the rostral PPE (Bailey et al., 2006; Schlosser and Ahrens, 2004).

Studies mostly performed in *Xenopus*, zebrafish and chick embryos have shown that the precursors of individual placodes are somewhat scattered within the PPE and partially intermingled with precursors of the adjacent placodes (Bhattacharyya et al., 2004; Bhattacharyya and Bronner, 2013; Dutta et al., 2005; Kozlowski et al., 1997; Pieper et al., 2011; Streit, 2002; Whitlock and Westerfield, 2000; Xu et al., 2008). The precise sequence of events that allows the transition from intermingled precursors within the PPE to the formation of well-defined individual placodes is still debated. However, cell displacement-promoting precursor coalescence and cell signalling-mediated (i.e. Nodal, Shh, Fgf, Bmp) acquisition of specific identities are two well-accepted mechanisms, which are thought to act in parallel or sequentially, depending on the favoured model (reviewed by Breau and Schneider-Maunoury, 2014; Breau and Schneider-Maunoury, 2015).

Most of the studies addressing rostral placode generation have focused on OP and LP (Bailey et al., 2006; Bhattacharyya et al., 2004; Bhattacharyya and Bronner-Fraser, 2008; Whitlock and Westerfield, 2000), leaving unresolved the issue of whether similar rules apply to the formation of the AHP. This placode is unique inasmuch as it is the only single placode and the only one that adopts neither a neurogenic nor a sensory fate but develops into a multi-hormone secretory gland: the adenohypophysis (Asa and Ezzat, 2004). Its specification, which is thought to occur no later than HH7/8 in chick embryos (ElAmraoui and Dubois, 1993), is known to require Nodal, Shh and retinoic acid signalling, and the activity of TFs such as Pitx2 and Lim3 (Devine et al., 2009; Dutta et al., 2005; Hatta et al., 1991; Herzog et al., 2003; Kondoh et al., 2000; Maden et al., 2007; Sheng et al., 1996; Zhao et al., 2006).

Fate-map studies in both zebrafish and chick embryos have established that, at neural plate stage, a restricted group of cells located in median PPE gives rise only to the AHP (Couly and Le Douarin, 1988; Dutta et al., 2005; Sánchez-Arrones et al., 2015). This could imply that AHP precursors occupy a special position within the PPE without intermingling with remaining placodal

[1]Centro de Biología Molecular Severo Ochoa, CSIC-UAM, c/ Nicolás Cabrera 1, Madrid 28049, Spain. [2]CIBER de Enfermedades Raras (CIBERER), c/ Nicolás Cabrera 1, Madrid 28049, Spain.

*Author for correspondence (pbovolenta@cbm.csic.es)

P.B., 0000-0002-1870-751X

Received 26 January 2017; Accepted 14 August 2017

Development (2017) 144, 3521-3532 doi:10.1242/dev.149724

precursors and/or that median-located PPE precursors had already initiated their specification toward an AHP fate at the time fate-map studies were performed, meaning specification occurred well before the time previously suggested (ElAmraoui and Dubois, 1993).

Here, we address these issues using the chick embryo as a model. We show that, in gastrulating embryos, AHP precursors are indeed largely segregated from the adjacent OL precursors and clustered at the midline, from where they hardly move. Median PPE precursors are superimposed on the underlying mesendoderm and soon express molecular features indicative of an endocrine organ, becoming molecularly distinct from the adjacent PPE precursors. We thus propose that adenohypophyseal placode precursors differ from the remaining PPE and speculate they might resemble other midline structures, e.g. the floor plate, which is important for maintaining the bilateral organization of the ventral neural tube (Bovolenta and Dodd, 1991).

RESULTS

AHP precursors localize at the median PPE largely segregated from OP precursors

In order to investigate how AHP precursors relate to the adjacent PPE cells, we first performed small DiI injections at different mediolateral positions of the PPE in HH4/5 chick embryos (n=67) and analysed the location of labelled cells at HH10-11, when the AHP, OP and LP can be easily recognized (Fig. 1A-L; Table S1). Using an overlying grid (Fig. 1A,E,I), we scored the initial position of the dye injections – distance from the node, angle from the midline, size of the injection – and the quantity and final location of labelled cells. Labelled cells were found in the rostral placodes, as well as in the rostral ectoderm and neural tissue (Table S1), given that at HH4/5 rostral PPE cells are not yet fully segregated from the neural and non-neural ectodermal cells (Sanchez-Arrones et al., 2012; Saint-Jeannet and Moody, 2014). The result of this analysis, focused exclusively on placodes, showed that, in HH4/5 embryos AHP precursors are mostly clustered at the median PPE (Fig. 1M). Indeed, cells originally positioned in the PPE region at a 6° angle from the midline, were found exclusively in the AHP (n=22 embryos; Fig. 1A-D; Table S1; Sánchez-Arrones et al., 2015). Intermingling between AHP and OP was observed only in embryos in which the dye was positioned at 7-9° (n=3), but, in this case, fewer labelled cells were recovered in the AHP (Fig. 1E-H; Table S1). Injections positioned in the rostrolateral PPE instead did not contribute to the AHP but were found in both the OP and LP (n=40; Fig. 1I-L, Table S1). Using this information, we estimated that the region occupied by AHP precursors spans an area of about 32,800 μm^2 (0.032 mm^2) at each side of the midline, with a limited intermingling with OP precursors. Analysis of labelling distribution further indicated that OP and LP precursors are more interspersed and occupy a larger area (Table S1; Fig. 1M). Notably, a similar analysis, scoring the rough position of labelled cells within the placodes of HH10/11 embryos – distance from the initial node position and final angle from the midline – indicated that AHP precursors barely move from the midline but displace anteriorly. This is perhaps expected given that the AHP is a midline structure that will end up positioning at the ventral embryonic side as the neural plate folds and bends. OP and LP precursors instead appeared to drift mostly mediolaterally (Fig. 1N).

To verify this different behaviour, we tracked the movements of individual rostral PPE cells by forcing the expression of the photo-convertible Kaede protein (Mendes et al., 2014) in the PPE of HH4/5 cultured embryos by means of electroporation (Fig. 2; Movies 1, 2). Time-lapse analysis of precursors photo-converted (red) in the rostrolateral PPE confirmed that all cells underwent directional medial-to-lateral movements during the subsequent 3 h of recording, mostly following independent paths that freely crisscrossed along the way (5/5 embryos; Fig. 2A-B′; Movie 1) (Toro and Varga, 2007). Cells were also observed to divide frequently, as further confirmed using BrdU-incorporation studies performed in HH4/5 embryos (212±27 lateral versus 127±18 median BrdU-positive cells, P=0.02; Fig. S1). When embryos were allowed to develop for an additional 18 h, photo-converted cells (with low fluorescence intensity due to recording photobleaching) were finally positioned in the OP and/or LP (Fig. 2C,D; inset). Additional and brighter cells (not photobleached) were found in the neural plate (Fig. 2C,D), likely because of the already mentioned lack of a sharp boundary between neural and non-neural cells in HH4/5 embryos, especially in lateral positions (Sanchez-Arrones et al., 2012). In contrast, median PPE cells underwent only short local movements, without apparent changes in their relative position even upon longer observation times (5/5 embryos; Fig. 2F-G; Movie 2). These cells were dividing at a significantly lower rate (Fig. S1) and were finally tracked exclusively in the AHP (Fig. 2H,I; inset).

Altogether, these data indicate that OP and LP precursors are initially interspersed in the rostral PPE and then separate by mediolateral displacement, a process that should contribute to their coalescence into defined placodes, as previously proposed (Bailey and Streit, 2006; Bhattacharyya et al., 2004; Bhattacharyya and Bronner, 2013). In contrast, the majority of AHP precursors are largely segregated from the remaining PPE cells and occupy a median position from the beginning of PPE specification.

Median and rostrolateral PPE cells present different morphological characteristics

The clustering of AHP precursors in the median PPE and their poor mobility, when compared with that of the adjacent progenitors, pointed to possible differential characteristics. To test this possibility, we compared the arrangement of median and rostrolateral PPE cells between HH4 and HH7/8 using scanning electron microscopy (SEM). In intact embryos, the rostral PPE can be easily identified as the tissue abutting the border of the anterior neural plate ridge (Fig. 3A,F,I,L). Cross-sections at the level of the rostral PPE (Fig. 3A-E) revealed that, in HH4 embryos (n=3), median cells were more elongated than the lateral ones with a cuboidal shape (compare Fig. 3D with 3E). Notably, this organization extended for about 180 μm at each side of the midline, coinciding with the zone occupied by AHP precursors, as estimated from data reported in Fig. 1M,N. At HH5/6 (n=2) and HH7/8 (n=3), these differences increased: median-located PPE cells became progressively compacted, elongated and bottle-shaped; these cells also appeared in close contact with the underlying axial mesendoderm (Fig. 3B,G,J,M). In contrast, laterally positioned rostral PPE cells remained rectangular in shape, forming a regularly organized epithelium that was quite separated from the underneath endodermal layer (Fig. 3C,E,H,K,N).

The distinct morphology of median versus rostrolateral PPE cells already at stage HH5 was confirmed by immunostaining with antibodies against β-catenin. z-projections of confocal images taken through the apical side of the rostral PPE – identified by the expression of the placodal marker *Tfap2a* (Kwon et al., 2010) (Fig. 4A-C) – highlighted a significantly smaller area and clustered organization for median cells (Fig. 4A,D). In contrast, laterally located cells presented an irregular and larger surface (Fig. 4B,D). Notably, staining with antibodies against the extracellular matrix protein laminin (Fig. 4E-G; Fig. S2) showed the virtual absence of a

Development (2017) 144, 3521-3532 doi:10.1242/dev.149724

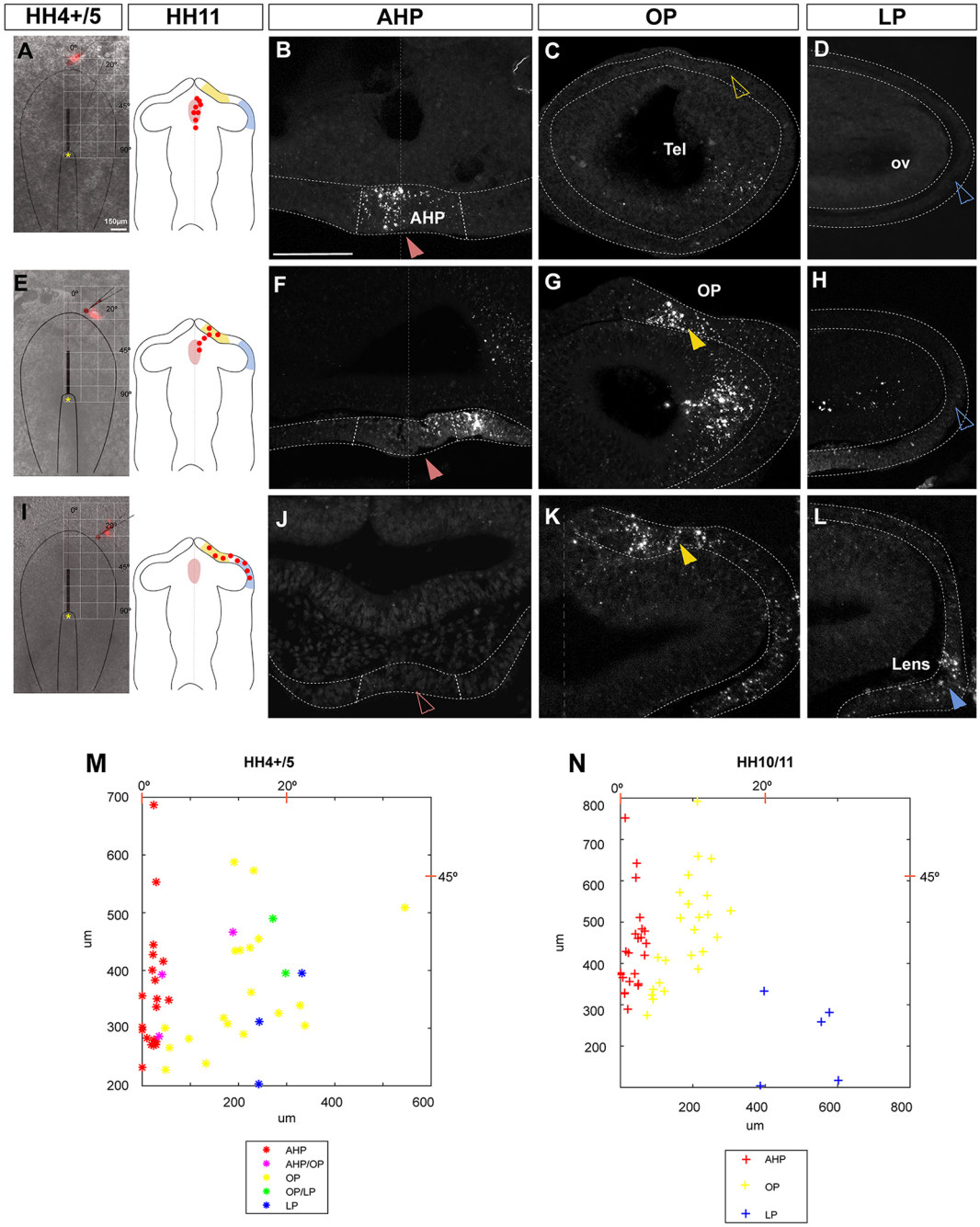

Fig. 1. Median-localized AHP precursors are segregated from the adjacent OP/LP precursors. (A,E,I) Images of embryos at HH4/5, when the injections were performed, with an over-layered schematic representation of the grid used to position the DiI injections (left). The grid was positioned so that the origin overlapped with the position of the Hensen's node (yellow asterisk) and the 0° reference (dotted red line) with the midline. On the right, schematic representation of ventral views of HH11 embryos indicating where labelled cells were found. The AHP, OP and LP are indicated in pink, yellow and blue, respectively. Red dots indicate DiI-labelled cells. (B-D,F-H, J-L) Transverse cryosections of representative embryos (HH11) showing the final position of labelled cells, following median (n=26; B-D) or rostrolateral (n=40; F-H,J-L) PPE labelling, as indicated in A,E,I. Sections were taken at the AHP, OP and LP levels, as indicated in the panels. Red, yellow and blue arrowheads indicate labelled cells in the AHP, OP and LP, respectively. The position of the AHP, OP and LP with no DiI-labelled cells in C, D, H and J is indicated with open color-coded arrowheads. The neuroepithelium is highlighted by dotted lines. (M,N) Polarplot distribution of initial (M) and final (N) distribution of DiI-labelled cells, taking into consideration their distance (µm) from Hensen's node (0) and their angle from the midline (0° coinciding with the y-axis). The plot represents only pre-placodal/placodal cells, although labelled cells contributed to neural and non-neural ectoderm (Table S1). The initial position of each injection is represented by an asterisk in M, colour coded according to its derivatives, as indicated in the graph legend. The average final position of the labelled cells is represented in N with colour-coded crosses. AHP, adenohypophysis placode; LP, lens placode; OP, olfactory placode; ov, optic vesicle; Tel, telencephalon. Scale bars: A, 150 µm; B-L, 100 µm.

well-defined basal lamina underneath the median PPE in HH5/6 embryos so that median PPE cells appeared superimposed to the underlying mesendoderm (Fig. 4E), as observed with SEM (Fig. 3J). A well-defined basal lamina between the ectoderm and their underlying layer was instead present at the level of the rostral neural border and neural plate (Fig. 4F,G; Fig. S2F). Basal lamina

Development (2017) 144, 3521-3532 doi:10.1242/dev.149724

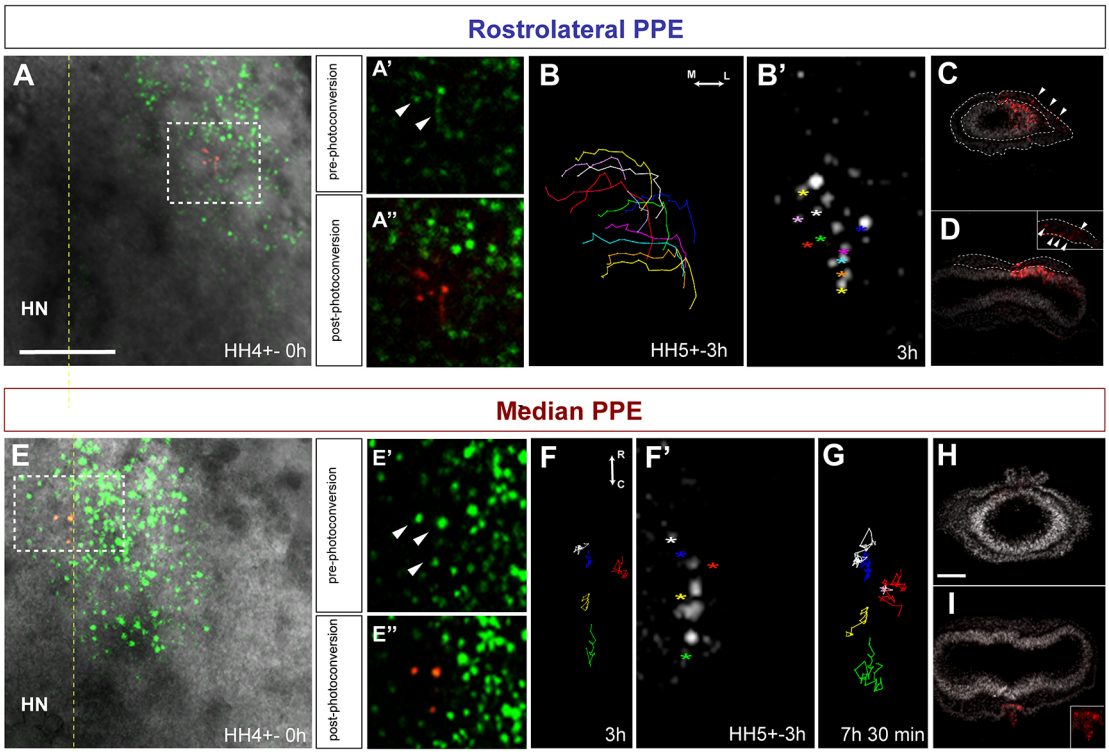

Fig. 2. Median-localized AHP precursors hardly move from the midline. (A-B′,E-G) High-power dorsal views of embryos recorded in Movies 1 and 2. The rostral PPE domain was electroporated at gastrula stage with a *kaede* expression plasmid. After 4 h, few Kaede-expressing cells positioned in the rostrolateral (A-A″; *n*=5) or median (E-E″; *n*=5) PPE were photo-converted to red. Their initial position is highlighted with white squares in A and E and with arrowheads in A′,A″,E′,E″. (B,B′,F,F′,G) Kymographs showing the change in position of 10 rostrolateral (B′) and 5 median (F′,G) cells during a recording period of 3 (B,F) and 7.5 (G) h. (B′,F′) Images of the position of recorded cells after 3 h (colour-coded asterisks). Rostrolateral cells move mediolaterally, median cells move only locally, even after protracted observation (G). (C,D,H,I) Transverse sections of recorded embryos, fixed at HH10 showing the final localization of the progeny of red Kaede-positive cells. Sections were taken at the OP (C,H), LP (D) and AHP (I) levels. Rostrolaterally derived cells localize at the OP (C), LP (D) and in the neural tissue, whereas medially derived cells were found only in the AHP (I,H). Owing to photobleaching during time-lapse, recorded cells are less fluorescent (arrowheads in C,D) and thus are shown in the insets in D and I at a higher exposure. HN, Hensen's node; m, l, medio-lateral; r, c; rostro-caudal. Scale bars: A 250 µm; H, 100 µm.

absence was observed in the central region of the presumptive area occupied by the AHP precursors as depicted in Fig. 1M.

In summary, median PPE cells differ from the adjacent OL/LP precursors in their shape and distance from the underlying mesendodermal tissue. These specific features of median PPE cells could reflect the existence of heterogeneity and/or lineage bias among rostral PPE precursors, as also suggested for OP and LP progenitors (Bhattacharyya and Bronner, 2013).

Median PPE cells begin to acquire an AHP character at the neurula stage

Given the morphological differences between median and rostrolateral PPE precursors, we next asked whether laterally located precursors could replace the median ones. To determine this, we ablated the median region of the PPE, leaving the underlying mesoendoderm intact (Fig. S3), at three different developmental stages (HH4, HH5/6 and HH7/8), and analysed the consequences at neural tube stage (HH11-13), when the AHP is morphologically and molecularly distinguishable thanks to the expression of Lim3 and *Pitx2* (Sánchez-Arrones et al., 2015; Sheng et al., 1996; Sjödal and Gunhaga, 2008). Ablations at HH4 had no apparent effect on AHP development (5/5 embryos; Fig. 5A-F), indicating that abutting cells can easily replace AHP precursors at this stage. In contrast, similar ablations at the head-fold stage (HH5/6) significantly reduced the size of the AHP rudiment (6/6 embryos; Fig. 5C,G-I). Consistent with previous reports (Cajal et al., 2014; Camus et al., 2000; ElAmraoui and Dubois, 1993), ablations at neurula stages (HH7/8) caused a stronger phenotype: the AHP was largely absent or formed only by a few Lim3-positive cells (5/5; Fig. 5C,J-L), and did not undergo the thickening and invagination observed in control embryos (5/5; Fig. 5A,B).

Therefore, at head-fold stages (HH5/6) median and lateral cells already differ so that rostrolateral precursors can no longer acquire a median character. To further assess this assumption, we looked at whether median and rostrolateral HH5 PPE cells express distinctive mRNA repertoires. To achieve this, we performed RNA-seq analysis (in triplicates) of HH5 median and rostrolateral PPE tissue (results are available at http://www.ebi.ac.uk/ena under accession number PRJEB21219), including the underlying mesendoderm (Fig. 6A). Comparative analysis of the obtained sequences revealed 239 differentially expressed mRNA with q>0.05. Of those, 186 were over-represented in median samples, whereas only 53 were significantly over-represented in rostrolateral ones (Fig. 6B). Validating our analysis, none of the mRNAs proposed to confer a rostral PPE ground state (i.e. *Six1*, *Six4*, *Eya1* and *Pax6*) was found to be enriched in either rostrolateral or median samples (Fig. 6C). The few mRNAs over-represented in the rostrolateral samples included those known to be thereafter expressed in the olfactory epithelium and/or the lens (Fig. 6C; Table S2), such as the TFs *Dlx5*, *Foxc2*, *Pax1* and *Sp8*, the secreted protein *Bmp5* and keratin genes (Bailey et al., 2006; Bhattacharyya et al., 2004; Kasberg et al., 2013). mRNAs over-represented in the median samples included those of the TFs *Hesx1*, *Six3* and *Six6*, the secreted ligands *Shh* and *Fgf3*, the

Development (2017) 144, 3521-3532 doi:10.1242/dev.149724

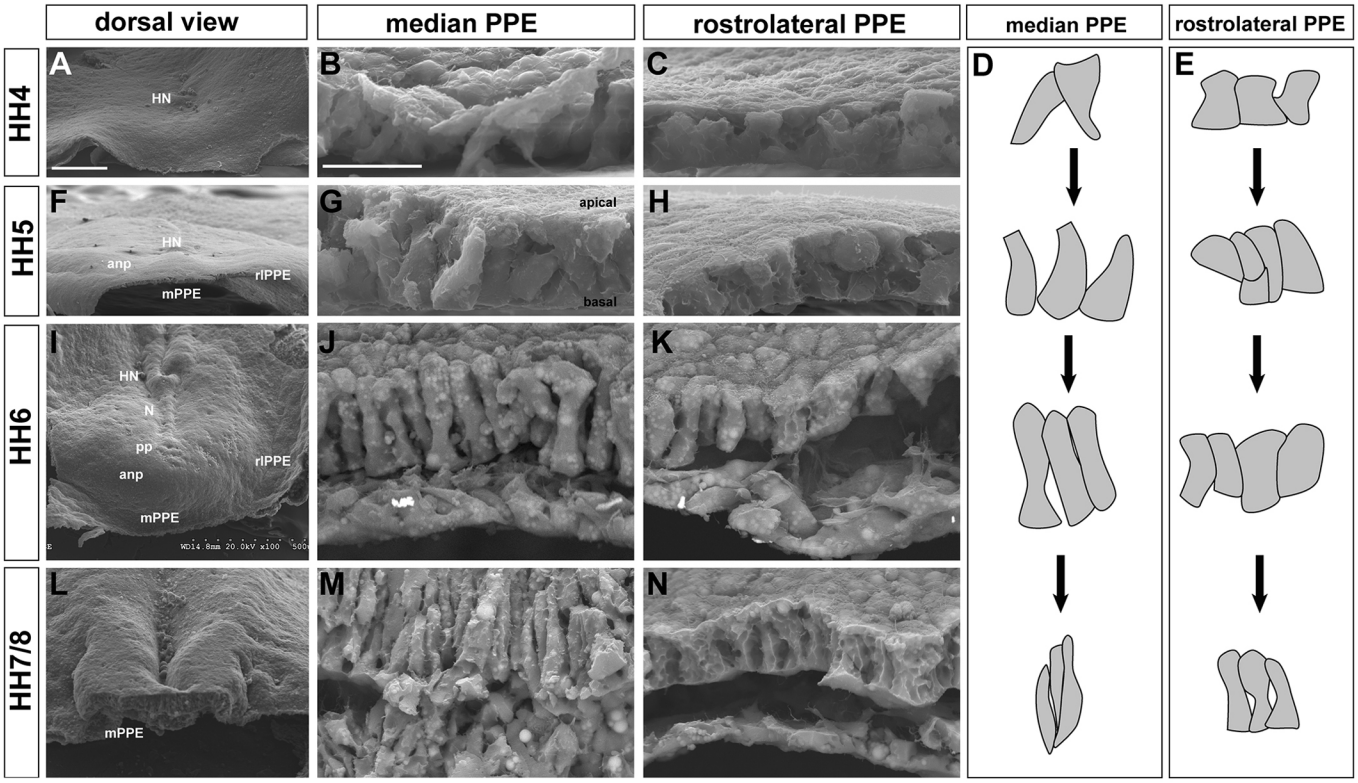

Fig. 3. Median and rostrolateral PPE cells are morphologically different. Images show dorsal (A,F,I,L) and transverse (B,C,G,H,J,K,M,N) scanning electron microscope views of stage HH4-7/8 chick embryos, as indicated in the panels. Transverse sections in B,G,J,M were taken at the median PPE, those in C,H,K,N at the rostrolateral level. Median and rostrolateral cells are morphologically different, as schematized in D,E. Note the close apposition of median (J,M) but not rostrolateral (K,N) PPE with the underlying mesendoderm. Three embryos for each stage in three independent experiments were analysed. anp, anterior neural plate; HN, Hensen's node; lrPPE, lateral rostral preplacodal ectoderm; mrPPE, median rostral preplacodal ectoderm; N, notochord; pp, prechordal plate. Scale bars: A, 250 µm; B, 20 µm.

hormone pro-opio-melano-cortin (POMC) and the corticotropin-releasing hormone (CRH) receptor (Fig. 6C, Table S2). Notably, these molecules have been shown to contribute to adenohypophysis patterning and/or differentiation (Beccari et al., 2012; Dattani et al., 1998; Gallardo et al., 1999; Guner et al., 2008; Herzog et al., 2004; Li et al., 2002; López-Ríos et al., 1999; Parkinson et al., 2010; Sajedi et al., 2008; Sbrogna et al., 2003), supporting the observation that median PPE cells are already biased towards an AHP fate at HH5. The mRNA of the neuroendocrine hormone somatostatin, which activates *Pax6* expression in the rostral PPE (Lleras-Forero et al., 2013), was also enriched in the median samples. Furthermore, the mRNAs of a number of other genes that, although not formally implicated in AHP patterning, might potentially contribute to this process were also over-represented in median samples (Table S2). For example, additional components of the Fgf signalling pathway, *Fgf19* and the signalling effector *Sprouty1*, were among those with the highest fold change in median versus rostrolateral explants. The Wnt and Bmp signalling inhibitors, *Dickkopf1* and *chordin*, were also of interest because the low activity of both signalling pathways is a requisite for rostral PPE specification (Kwon et al., 2010; Litsiou et al., 2005). *ApoB*, the mRNA of which was the most over-represented in medial samples, may facilitate Shh signalling in zebrafish development and its knockdown causes midline defects (Seth et al., 2010). The TFs *Lmx1a* and *Lhx1* were also notable candidates as both are expressed in the AHP at later developmental stages (http://geisha.arizona.edu/geisha/).

To validate these transcriptional profiles, we performed *in situ* hybridisation for a few of the identified mRNAs (Fig. 6D). From head-fold stages, the expression of both *Lhx1* and *Lmx1a* was restricted to the median PPE, overlapping with that of the Shh receptor *Ptch2* (Fig. 6D), another of the medially over-represented mRNAs (Table S2), which is specifically expressed in the chick AHP at later stages (Sjödal and Gunhaga, 2008). Notably, we were unable to detect a 'rostrolateral PPE-specific' distribution for any of the mRNAs differentially expressed in the rostrolateral samples (Table S2), with the exception of the transcription factor *Sp8*. Its mRNA was completely absent from the median PPE at head-fold stages but abundantly expressed in the remaining PPE (Fig. 6D). Therefore, according to this analysis, AHP precursors can be recognised for being *Lhx1*, *Lmx1a* and *Ptch2* positive and *Sp8* negative, which represents a specific molecular signature within the PPE at early developmental stages.

Notably, several cell-adhesion molecules were also over-represented in the medial samples (Table S2). This was of particular interest as a greater adhesion among precursors or with the underlying mesendoderm (included in the samples) could, at least in part, explain the limited cell movements observed in the AHP precursors (Figs 1 and 3G,J; Movie 1). Indeed, the expression of two of the most enriched cell-adhesion molecules, *Cdh20* and *Cdh6*, specifically localised to the median mesendodermal layer (Fig. 6D; data not shown).

Taken together, these data indicate that the rostral PPE is already molecularly and morphologically heterogeneous at HH5/6. Indeed, differential gene expression, shape, organization and close apposition with the mesendoderm distinguished the median-located AHP cells from the rostrolateral precursors.

Development (2017) 144, 3521-3532 doi:10.1242/dev.149724

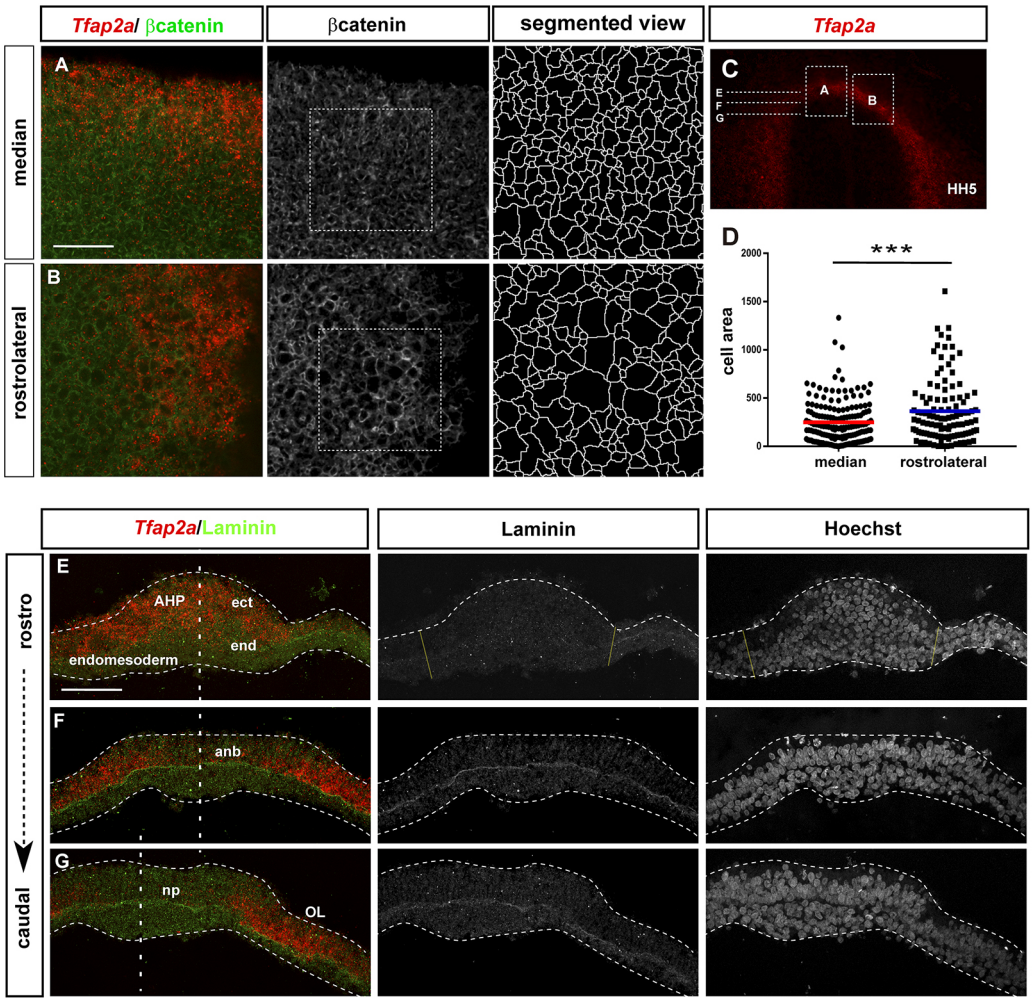

Fig. 4. Median and rostrolateral PPE cells are differentially organized. (A-C) Dorsal views of the median and rostrolateral PPE in HH5 embryos (*n*=6 for experimental group) hybridized *in toto* for the PPE marker *Tfap2a* and immunostained for β-catenin. The regions magnified in A and B, and the levels of the sections E-G are indicated in C. Median cells are smaller and more densely packed than those in the rostrolateral PPE cells, which are better appreciated in the segmented views. (D) Quantification of the median and rostrolateral cell area in a representative embryo. Student's *t*-test; ****P*=0.000569. Single-cell area was determined in regions of 5000 μm^2 of either the median or rostrolateral PPE in six embryos, obtaining similar results. (E-G) Frontal sections of HH5 embryos hybridized *in toto* for *Tfap2a* and immunostained for laminin. No signal is detected underneath the prospective AHP (E). Dashed lines in E-G indicate the midline. AHP, adenohypophysis placode; anb, anterior neural border; ect, ectoderm; end, endoderm; np, neural plate; OL, olfactory placode. Scale bar: 50 μm.

Median PPE precursors can be replaced by both lateral PPE and neural ectoderm

The distinctive features of median PPE cells made us wonder whether rostrolaterally positioned PPE cells would be competent to fully substitute for the median ones; or if the abutting median neural or non-neural ectodermal cells were a more likely replacement for the median PPE. This possibility seemed plausible as the PPE forms at the interface between the neural and non-neural ectoderm (Bailey and Streit, 2006; Baker and Bronner-Fraser, 2001; Couly and Le Douarin, 1988; Streit, 2004), concomitant with the sharpening of the anterior neural border, where median-positioned cells move along the rostrocaudal axis (Cajal et al., 2012; Sanchez-Arrones et al., 2012), as AHP precursors do (Fig. 1; Sánchez-Arrones et al., 2015). In other words, we wondered whether the 'preplacodal' character prevails over the 'median' character (or vice versa).

To address this issue, we performed additional ablations of the median PPE in HH4 embryos but, this time, we concomitantly labelled cells immediately adjacent to the ablated region with DiI and DiO. In a first set of experiments, we placed the dyes lateral to the ablation, so that rostrolateral precursors from the right hemi-side were labelled in red and those from the left in green (Fig. 7). In ablated embryos, labelled cells appeared to move in both medial and lateral directions, soon replenishing the missing tissue (Fig. 7C,C′, G,G′), forming a normal AHP, as confirmed by the localization of green- and red-labelled cells in HH11 embryos (5/6 embryos; Fig. 7K). Notably, red- and green-labelled cells intermingled in the AHP, indicating that cells derived from the left hemi-side crossed the midline invading to the right AHP and vice versa, a behaviour never observed in non-ablated embryos (Fig. 7A-D′,E-F′,I,J), in which neither median or lateral cells (23/25; Fig. 7A-B′,E-F′,I-J) were labelled.

In a second set of experiments, dyes were placed rostrally and caudally to the ablated region, thus labelling the non-neural and neural ectoderm, respectively. Subsequent analysis of the embryos at stage HH6/7 and HH11 clearly demonstrated that only neural-derived DiI-labelled cells contribute to replenish the ablated region, whereas DiO-labelled ectodermal cells moved dorsally, away from the ablated region (5/5 embryos; Fig. 7D,D′,H,H′,L).

Development (2017) 144, 3521-3532 doi:10.1242/dev.149724

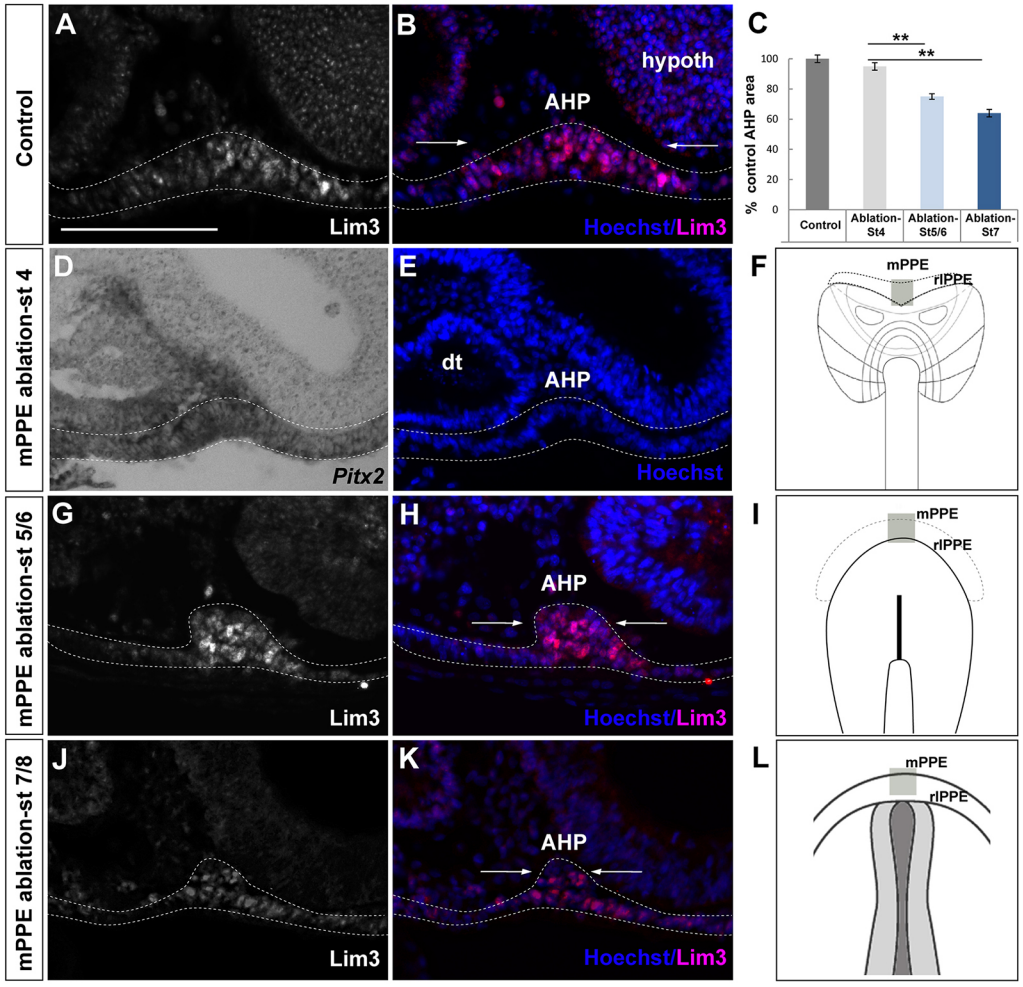

Fig. 5. Rostrolateral PPE precursors no longer replace AHP precursors after head-fold stages. Mid-sagittal sections of HH11-13 control (A,B) and experimental (D,E, G,H,J,K) embryos in which the median PPE was ablated at HH4 (D, E), HH5/6 (G,H) and HH7/8 (J,K), as schematized in F,I,L. The ablated region is indicated by a grey rectangle. Sections were immunostained for Lim3 or hybridized for *Pitx2*, as indicated in the panels. Sections in B,E,H,K were counterstained with Hoechst. Dashed lines outline the AHP. Ablations at HH5/6 strongly reduced the AHP size (G,H). (C) Quantification of the AHP area in control (n=5) and ablated (n=5) embryos (**P<0.01, Student's t-test; data are mean±s.e.m.). AHP, adenohypophysis placode; hypoth, hypothalamus; rlPPE, rostrolateral preplacodal ectoderm; mPPE, medial preplacodal ectoderm. Scale bar: 200 µm.

Taken altogether, these data suggest that median PPE precursors can be replaced by both cells of rostral neural origin and adjacent PPE precursors. The latter, however, freely cross the midline, a behaviour not observed in AHP precursors.

DISCUSSION

In gastrulating vertebrate embryos, a fringe of ectodermal tissue in between the newly specified neural ectoderm and the adjacent non-neural ectoderm hosts interspersed cells that will finally sort out to originate individual cranial placodes and neural crest cells (Saint-Jeannet and Moody, 2014). Our study shows that AHP precursors represent an exception to this initial arrangement, because, from the very beginning of PPE specification, these cells are packed together and abut the underlying mesendoderm. Localized at the PPE midline, they hardly move or mix with the adjacent rostrolateral PPE precursors, very soon acquiring a specific molecular signature, including the expression of genes characteristic of their final AHP fate, which distinguishes them from the remaining PPE. Upon ablation, AHP precursors can be replaced, albeit with a greater plasticity, by the adjacent PPE precursors and by midline neural cells, raising the interesting, yet to be tested, possibility that, besides originating the anterior adenohypophysis, these cells may have the additional purpose of acting as an axial reference to maintain PPE mirror-symmetry.

The extent to which precursors of individual placodes are intermingled within the PPE is still a matter of debate. Initial studies based on fate maps and DiI labelling suggested extensive mixing among different precursors (Bhattacharyya et al., 2004; Streit, 2002; Xu et al., 2008), but subsequent studies indicated that this had been probably overestimated, being prominent mostly at boundaries between adjacent placodal progenitor zones (Pieper et al., 2011; Schlosser, 2014). Our results, based on analysis of DiI-labelled cells, support the existence of intermingling and cell displacement for OP and LP precursors. Time-lapse studies indicated that this displacement was mediolaterally directed, although we cannot exclude that part of the cells we followed were neural in origin. Indeed, at the time of PPE labelling, neural cells are still intermingled with non-neural cells, especially in lateral positions (Sanchez-Arrones et al., 2012), in agreement with the final localization of photoconverted cells also in neural tissue. Nevertheless, mediolateral displacement of OP and LP precursors is also inferred from the DiI-labelling experiments and it is well in agreement with a recent study performed in *Xenopus* embryos (Steventon et al., 2016). In contrast, the majority of AHP precursors underwent only short local movements and were segregated from the adjacent OP/LP progenitors (Fig. 1). As an exception, laterally positioned AHP precursors, which were thereafter found in the most lateral regions of the AHP, partially intersperse with the OP ones (Fig. 1). This organization resembles that of the zebrafish with an extensive mixing of OP/LP precursors and a prominent presence of AHP precursors at the midline (Dutta et al., 2005). Therefore, the rostral chick PPE seems composed of two different pools of cells, at least in terms of their segregation and mobility. Median PPE cells begin to express genes that are thereafter found in the differentiating

Development (2017) 144, 3521-3532 doi:10.1242/dev.149724

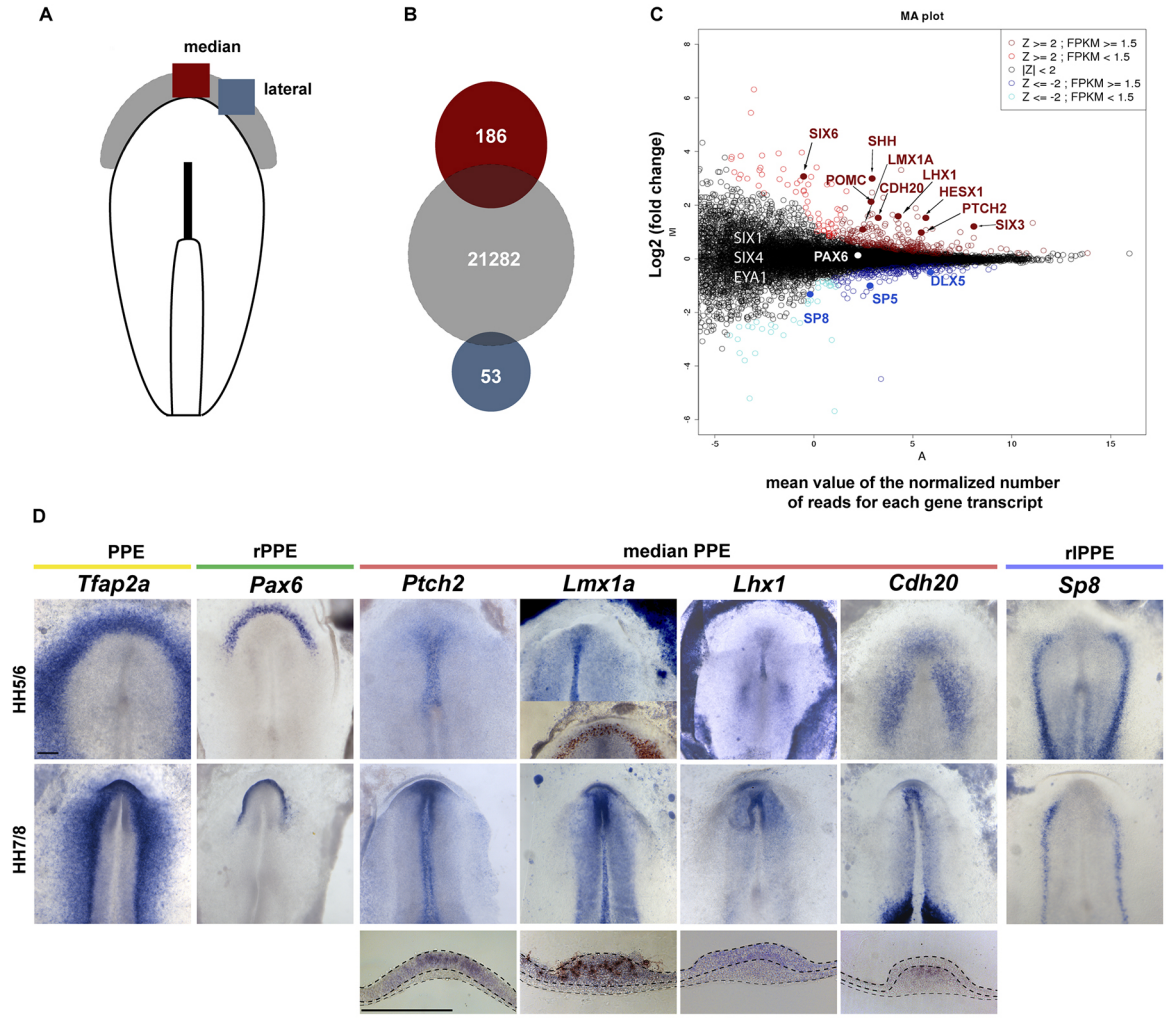

Fig. 6. The median and rostrolateral PPE are molecularly distinct at head-fold stage. (A) Schematic representation of a HH5/6 chick embryo in which the rostral PPE is depicted in grey and the median and rostrolateral PPE regions used for RNA-seq analysis are depicted in red and blue, respectively. A total of 150 median and 300 rostrolateral PPE were dissected. (B) Schematic representation of the RNA-seq results, indicating the number of non-differentially expressed (grey) and median (red) or lateral (blue) over-represented mRNAs. (C) Scatter diagram of mRNA representation in median and rostrolateral samples. Black, red and blue dots represent mRNA equally expressed in both domains, or significantly enriched in median or rostrolateral samples, respectively. (D) Dorsal views of HH5/6 and HH7/8 chick embryos hybridized *in toto* with probes specific for a few identified mRNA, as indicated in the panels. *Lmx1a* is also represented in a double *in situ* with *Tfap2a* (brown staining). Images in the bottom row are transverse sections at the level of median PPE. There is restricted expression of selected markers. PPE, pre-placodal ectoderm; rPPE, rostral pre-placodal ectoderm; rlPPE, rostrolateral pre-placodal ectoderm. Scale bar: 200 µm.

adenohypophysis only with a few hours difference from PPE specification. Thus, it is experimentally difficult to establish whether this is always so, or whether lack of mobility represents a feature related to the onset of the AHP character. The early morphological difference between rostrolateral and median PPE cells calls for intrinsic differences among precursors. This is supported by previous studies showing a midline-restricted displacement of median-positioned cells also at earlier stages, when sharpening of the neural non-neural boundary is taking place in the chick embryo (Sanchez-Arrones et al., 2012).

There might be several reasons for the existence of a specialised pool of AHP precursors, including the fact that the AHP is the only single placode and the only one with an endocrine character. Another reason might be their midline position. Median PPE ablations allow for abnormal midline crossing of rostrolaterally PPE cells. This behaviour may simply reflect the need to repair the wound or could be a consequence of the intrinsic higher motility of the rostrolateral PPE. In a more speculative view, the greater adhesion and less mobility of median-located PPE precursors might lead them to act as an axial reference to maintain a symmetric organization of the PPE. Indeed, in *Shh* mouse mutants, in which the AHP fails to be specified, OP symmetry is lost (Chiang et al., 1996). In all chordates, midline cells have the fundamental role of establishing a mirror-symmetry of the body plan (Ruiz i Altaba and Jessell, 1993), which is associated with specific features, including poor proliferation and high adhesion (Klar et al., 1992; van Straaten et al., 1988), as we report for median PPE cells. Cell division is a major driver of cell rearrangements, whereas poor proliferation stabilizes the tissue, as suggested in a study addressing how epithelial cells rearrange during chick embryo gastrulation (Firmino et al., 2016). Thus, the less mitotically active median PPE may offer a stable axial reference to the adjacent cells, favouring their movements. This stability could be further enhanced by the absence of a clear basal lamina between the central region of the median PPE and the underlying *Cdh6*- and *Cdh20*-enriched mesendoderm. Whether this arrangement is relevant is just a matter of speculation

Development (2017) 144, 3521-3532 doi:10.1242/dev.149724

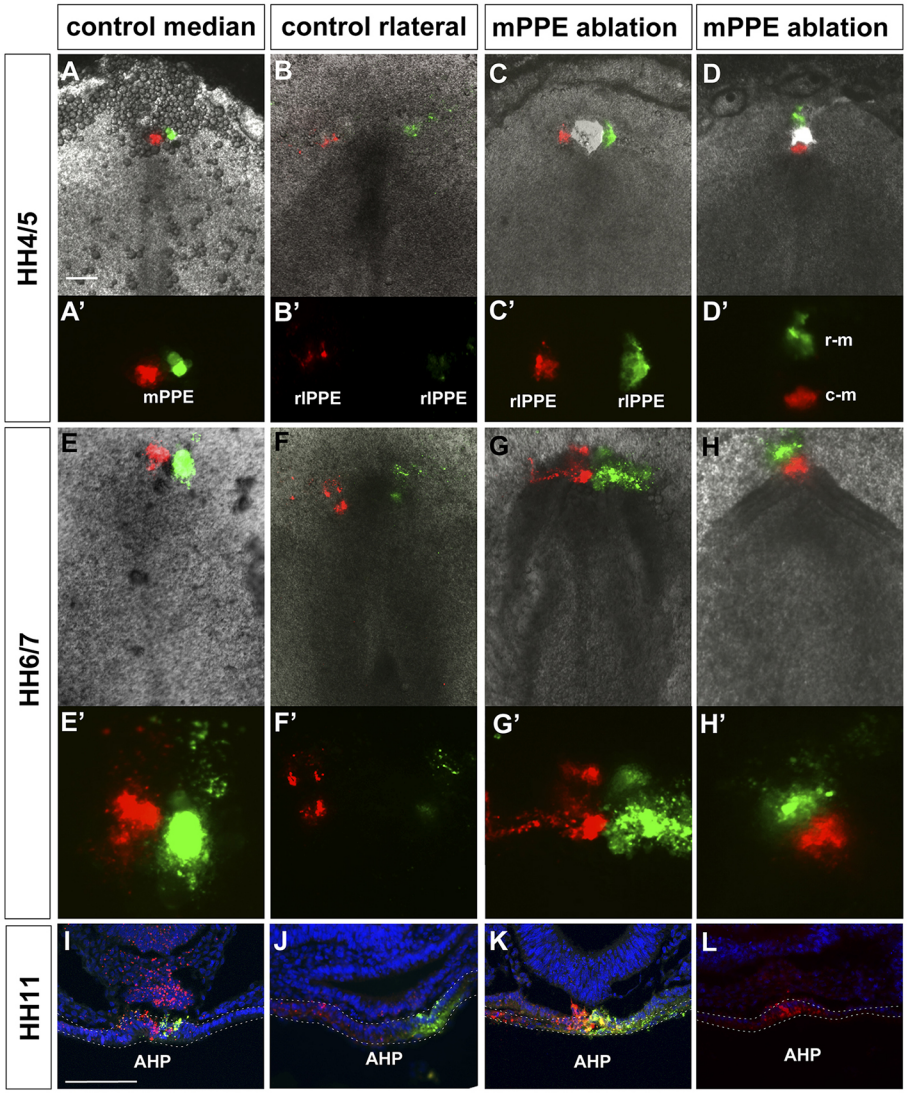

Fig. 7. Median PPE precursors can be replaced by both rostrolateral PPE and neural ectodermal cells. Phase contrast (A-D) and fluorescent (A′-D′) dorsal views of HH4/5 embryos with or without ablation of the median PPE, followed by DiI and DiO labelling of the adjacent lateral (*n*=6) or dorso/ectodermal-ventral/neuroepithelial (*n*=5) cells, as indicated in the panels. Phase contrast (E-H) and fluorescent (E′-H′) dorsal views of the same embryos grown at HH6/7 showing how lateral (G,G′) and neuroepithelial (H,H′), but not ectodermal, cells replenish the ablated tissue. (I-L) Transverse sections of the AHP from the same embryos grown at HH11. In controls, left/DiI- and right/DiO-labelled cells remain in the hemi-side, whereas in ablated embryos left- and right-derived cells intermingle (I). Only neuroepithelial-derived DiI-labelled cells contribute to the AHP (L). AHP, adenohypophysis; c-m, caudo-median; rlPPE, rostrolateral preplacodal ectoderm; mPPE, median preplacodal ectoderm; r-m, rostro-median. Scale bars: 100 µm.

at the moment, because we were unable to target the axial mesendoderm, in an attempt to disrupt its putative contact with the PPE, using electroporation of available dominant-negative *Cdh20* constructs (Price et al., 2002).

We have shown that, upon ablation at late gastrula stage, the abutting PPE precursors can replace the presumptive AHP. The identity of the replenishing cells cannot be established with precision at this early stage owing to the lack of reliable specific markers. Presumably these cells could be OP precursors, which intermingle at the border of the presumptive AHP domain and share some of their features. Indeed, the adenohypophysis and the olfactory organ of the lamprey are closely associated (Uchida et al., 2003), and in zebrafish, AHP and OP express common molecular markers (Dutta et al., 2005; Toro and Varga, 2007). Alternatively, these cells may derive from the few AHP precursors intermingled at the boundary with OP cells (Fig. 1). Previous studies in both zebrafish and chick indicate that, despite their intermingling, the large majority of single rostral PPE precursors are strongly biased and can originate only one placodal fate (Bhattacharyya and Bronner, 2013; Dutta et al., 2005; Whitlock and Westerfield, 2000).

The ablated median PPE was replaced also by median-located neural cells. According to fate-map analysis, the chick AHP has a strict extra-neural origin (Sánchez-Arrones et al., 2015). This may make our result surprising. However, timing of ablation may be important when interpreting this result. Indeed studies in *Xenopus* have shown that both the neural and non-neural ectoderm are competent to generate the PPE, but in the case of the neural tissue this competence drops over time (Pieper et al., 2011). The relationship between median PPE and median-located neural cells might be also linked to their responsiveness to Shh signalling, as indicated by their common expression of *ptch2* (Fig. 5).

Besides showing that prospective AHP cells have morphological features that distinguish them from the adjacent PPE precursors, our study demonstrates that these cells begin to express a specific genetic repertoire around HH5/6, when adjacent cells can no longer replace them upon ablation. This molecular signature includes adenohypophysis differentiation markers such as the hormone POMC or the CRH receptor, a number of secreted molecules and TFs known to contribute to AHP development and differentiation, as well as the lack of *Sp8* expression. This TF was distributed throughout the PPE but in its median region, thus becoming a valuable marker to differentiate between the prospective AHP domain and the remaining placodal precursors. More importantly, our RNA-seq analysis identified potential additional components of the gene regulatory network responsible for AHP specification and differentiation, which have not been so far considered. The TFs Lhx1 and Lmx1a might be

Development (2017) 144, 3521-3532 doi:10.1242/dev.149724

of particular interest. In mouse embryos, *Lhx1* is essential for gastrulation and its genetic inactivation causes early lethality (Shawlot and Behringer, 1995; Shawlot et al., 1999), precluding the analysis of its possible role in AHP specification. However, conditional inactivation of *Lhx1* in the epiblast showed that its function is essential for midline morphogenesis (Costello et al., 2015). Furthermore, Lhx1 binds and activates the regulatory region of *Hesx1* (Chou et al., 2006), maintaining its expression (Costello et al., 2015). Thus, it is tempting to speculate that Lhx1 might have similar functions in the midline-positioned AHP, the development of which requires *Hesx1* (Dattani et al., 1998). Much less is known about the possible function of *Lmx1a* during early embryonic development. *Lmx1a* acts downstream of Shh signalling in the specification of a number of hindbrain and cerebellar neurons (Chizhikov et al., 2010; Mishima et al., 2009), raising the possibility that its function might be also activated in the AHP by this signalling.

In conclusion, we propose that, by virtue of their position at the PPE midline, AHP precursors adopt characteristics that set them apart from the remaining PPE precursors. These features might be imposed by spatial constrains, perhaps interaction with the underlying mesendoderm and early exposure and response to midline signals such as Shh or Nodal. Whether similar restrictions apply to other placodal progenitors needs to be clearly determined but the existence of a lineage bias that precedes segregation has been recently proposed for chick OP and LP (Bhattacharyya and Bronner, 2013). Our study also emphasises that in an apparently homogeneous population of precursor cells there is an early cellular and molecular heterogeneity, which might be relevant to further understand the rare congenital defect associated to the adenohypophysis development (Prince et al., 2011).

MATERIALS AND METHODS

Chick embryos and embryo cultures

Fertilized chick embryos (Santa Isabel Farm, Cordoba, Spain) were incubated at 38°C in a humidified rotating incubator until the desired stage. Embryos were inspected for normal development, staged according to Hamburger and Hamilton (1951) and randomly allocated to the different experimental groups. Poorly developed embryos were discarded at any time during the course of the experiments. When needed, embryos were cultured according to the 'New culture method' (Stern and Bachvarova, 1997), starting from a minimum of 30-40 embryos to assure that at least 10 embryos finally met appropriate conditions for analysis. Each type of experiment was independently repeated at least three times. The precise position of median and lateral rostral PPE was identified using a calibrated ocular grid (Sánchez-Arrones et al., 2015). All experiments were performed according to European and Spanish guidelines for animal experimentation ethical regulations.

DiI/DiO injections

Fate-mapping experiments were performed in HH4/5 New-cultured chick embryos using DiI/DiO injections, which were precisely positioned using an ocular grid displaying cartesian and angular coordinates centred on the node. This allowed us to score the distance from the node, the angle from the midline and the size for each one of the injections (Table S1; Sanchez-Arrones et al., 2012), which were also photographed under fluorescent illumination. Embryos were cultured until HH10-12 stages, fixed in 4% paraformaldehyde (PFA) in 0.1 M phosphate-buffered saline (PBS) (pH 7.4) at 4°C and the presence and abundance (defined as +, ++ or +++) of labelled cells in the AHP, OP and LP were recorded in whole-mount embryo and transverse cryosections (Table S1).

Tissue ablations

The presumptive median PPE zone was removed at stages HH4, HH5/6 and HH7/8 using insect pins. Embryos were allowed to develop until they reached stage HH11-13, fixed as above, cryo-protected overnight in 15% sucrose solution in PBS and cryosectioned in the sagittal plane at 15 µm.

BrdU labelling

New-cultured embryos were incubated in a BrdU solution (10 µM) for 1 h, washed in PBS and fixed in ice-cold 4% PFA. Embryos were processed for *in toto* immunolabelling using a mouse monoclonal antibody against BrdU (1:200; Hybridoma Bank, G3G4) as described previously (Trousse et al., 2001).

Electroporation and time-lapse imaging

The pCAGGS-Kaede-NLS vector (1 mg/ml; Mendes et al., 2014) was electroporated in HH3+/4 New-cultured embryos (Voiculescu et al., 2008). Kaede photo-conversion was obtained by illuminating the region of interest with a UV (405 nm) laser beam for 10-20 interactions. The behaviour of labelled cells was followed with time-lapse confocal microscopy using a dry 20×0.8 NA objective for 8 h, taking one image every 5 min.

In situ hybridization and immunohistochemistry

Embryos were hybridized *in toto* as described (Sánchez-Arrones et al., 2015) using probes specific for the following chick mRNAs: *Shh*, *Ptc2*, *Hesx1*, *Pax6*, *Lhx1* (gifts from L. Medina, University of Lleida, Spain), *Cdh20* (a gift from C. Redies, University of Jena School of Medicine, Germany) and *Sp8* (a gift from Dr J. J. Sanz-Ezquerro, CNB-CSIC, Madrid, Spain). Probes for *Tfpa2a* and *Lmx1a* were obtained by RT-PCR amplification from cDNA of HH24 embryos with the following primers: *Tfap2a* fwd, 5′-ATGCTCTGGAAGCTGACGG-3′; *Tfap2a* rev, 5′-CGGTGACGGCAG CGCATAC-3′; *Lmx1a* fwd, 5′-GGACGGCTTGAAGATGGAGG-3′; *Lmx1a* rev, 5′-ATGCTCAGGAGGTGAAGTAG-3′. Immunohistochemistry was performed following standard protocols on cryostat sections or intact embryos. Primary antibodies used were as follows: mouse monoclonal against Lim3 [1:100; Hybridoma Bank, 67.4E12; (Prince et al., 2011)], ZO-1 (1:300; Invitrogen, 33-9100; clone, ZO1-A12) and β-catenin (1:500; Abcam, ab16051); and rabbit antiserum against laminin (1:100; Sigma, L-9393). Appropriate secondary antibodies coupled to either Alexa-488, -594 or -647 (Jackson ImmunoResearch, 1:500) were used. Sections were counterstained with Hoechst (1:1000; Molecular Probes) and mounted with Mowiol.

RNA-seq analysis

A total of 150 median and 300 lateral rPPE regions were dissected from HH5/6 chick embryos. These regions were divided in three different pools, and processed and sequenced in parallel in order to obtain experimental triplicates. A total of 1 µg of RNA per sample was extracted using ReliaPrep RNA Tissue Miniprep System Protocol (Promega). RNA quality was determined with RNA Analysis Kit and a Bioanalyzer (Agilent) (RIN>8). Separate mRNA libraries were prepared using the mRNA-Seq Sample Preparation kit (Illumina, RS-122-2001x2), according to the manufacturer's protocol. First-strand cDNA synthesis using random hexamers and reverse transcriptase was followed by second-strand cDNA synthesis. Quality analysis was performed over reads using FastQC software (http://www.bioinformatics.babraham.ac.uk/projects/fastqc/). Each library was sequenced using the HiSeq2000 instrument (Illumina). Reads were aligned against the reference *G. gallus* genome (gga_ref_Gallus_gallus-4.0), downloaded from NCBI (http://ftp.ncbi.nih.gov/genomes/Gallus_gallus/), with TopHat aligner (http://tophat.cbcb.umd.edu). Differentially expressed genes were identified with Cuffdiff (http://cufflinks.cbcb.umd.edu/index.html) software. A total of 239 genes were found as differentially expressed with a P-value ≤0.05. Of these 186 and 53 were medial and laterally overrepresented, respectively. Genes were selected when their log2 fold change was higher than 1 (absolute value). Data have been deposited in the European Nucleotide Archive with the following accession numbers: ERS1781601-ERS1781612.

Scanning electron microscopy (SEM)

Embryos at the desired stages were washed in saline to remove yolk and vitelline membrane, fixed for 2 h in 4% glutaraldehyde in 0.1 M sodium cacodylate buffer at room temperature and processed as described previously (Bancroft and Bellairs, 1976). Samples were analysed with a

Development (2017) 144, 3521-3532 doi:10.1242/dev.149724

SEM Hitachi S-3000N equipped with an INCAx-sight energy-dispersive X-ray (EDX) analyser (Oxford Instruments).

Image analysis

Whole embryos were photographed using a stereomicroscope and sections using a DM microscope (Leica Microsystems). Digital images were obtained using DFC500 and DFC350 FX cameras (Leica) or using confocal microscopic analysis (Zeiss). Images were processed using Photoshop CS5, Illustrator CS5 or ImageJ (Fiji) software. Representative images were used as imported templates in Adobe Illustrator to draw vectorial schemes.

Quantification and statistical analysis

Quantitative analysis of all experiments was performed using Image J (NIH), using only well-developed embryos. Differences between averages were considered significant when $*P<0.05$, $**P<0.01$, $***P<0.001$ using Student's *t*-test. The fate-map analysis shown in Fig. 1M,N was obtained with the MATLAB software using the 'polarplot' function and using as coordinates the initial and final angles and distances from the node reported in Table S1. The estimate of the PPE region occupied by AHP precursors was determined by calculating the area contained between the two arcs, in which the injections originating labelled cell in the AHP fell, according to the formula: total area=πr^2_{max} (angle/360)−πr^2_{min} (angle/360).

Acknowledgements

We are grateful to Florencia Cavodeassi, Pilar Esteve and Elisa Marti for critically reading the manuscript. We are indebted to Leonor Saúde, Loreta Medina, Stefan Price, Cristoph Redies and Jose Sanz-Ezquerro for providing reagents, and to the CBMSO Image Analysis and Genomic Services, in particular Maria Angeles Muñoz-Alcala and Ramon Peiró for their excellent technical assistance. We also wish to acknowledge Alessandro Rodriguez-Bovolenta for his help in generating Fig. 1M,N and Noemi Tabanera for editing the figures and generating the graph in Fig. 4C.

Competing interests

The authors declare no competing or financial interests.

Author contributions

Conceptualization: L.S.-A., M.J.C., P.B.; Methodology: L.S.-A., A.S., M.J.C.; Validation: A.S.; Formal analysis: L.S.-A., P.B.; Investigation: L.S.-A., A.S., M.J.C.; Writing - original draft: L.S.-A., P.B.; Writing - review & editing: P.B.; Supervision: P.B.; Project administration: P.B.; Funding acquisition: P.B.

Funding

This work was supported by the Secretaría de Estado de Investigación, Desarrollo e Innovació (MINECO), Spain (BFU2013-43213-P, BFU2016-75412-R and BFU2014-55738-REDT), the Comunidad Autonoma de Madrid (S2010/BMD-2315) and the Centro de Investigación Biomédica en Red de Enfermedades Raras (CIBERER) del Instituto de Salud Carlos III (ISCIII) to P.B. and by an institutional grant from the Fundacion Ramon Areces. L.S.-A. was supported by a postdoctoral contract from the Consejo Superior de Investigaciones Científicas (JAEDOC-012) and the Programa de Formación Postdoctoral from MINECO. M.J.C. was supported by a predoctoral contract from MINECO (BES-2008-005457).

Data availability

Data have been deposited in the European Nucleotide Archive under the accession number PRJEB21219.

Supplementary information

Supplementary information available online at
http://dev.biologists.org/lookup/doi/10.1242/dev.149724.supplemental

References

Asa, S. L. and Ezzat, S. (2004). Molecular basis of pituitary development and cytogenesis. *Front. Horm. Res.* **32**, 1-19.

Bailey, A. P. and Streit, A. (2006). Sensory organs: making and breaking the pre-placodal region. *Curr. Top. Dev. Biol.* **72**, 167-204.

Bailey, A. P., Bhattacharyya, S., Bronner-Fraser, M. and Streit, A. (2006). Lens specification is the ground state of all sensory placodes, from which FGF promotes olfactory identity. *Dev. Cell* **11**, 505-517.

Baker, C. V. H. and Bronner-Fraser, M. (2001). Vertebrate cranial placodes I. Embryonic induction. *Dev. Biol.* **232**, 1-61.

Bancroft, M. and Bellairs, R. (1976). The development of the notochord in the chick embryo, studied by scanning and transmission electron microscopy. *J. Embryol. Exp. Morphol.* **35**, 383-401.

Beccari, L., Conte, I., Cisneros, E. and Bovolenta, P. (2012). Sox2-mediated differential activation of Six3.2 contributes to forebrain patterning. *Development* **139**, 151-164.

Bhattacharyya, S. and Bronner, M. E. (2013). Clonal analyses in the anterior pre-placodal region: implications for the early lineage bias of placodal progenitors. *Int. J. Dev. Biol.* **57**, 753-757.

Bhattacharyya, S. and Bronner-Fraser, M. (2008). Competence, specification and commitment to an olfactory placode fate. *Development* **135**, 4165-4177.

Bhattacharyya, S., Bailey, A. P., Bronner-Fraser, M. and Streit, A. (2004). Segregation of lens and olfactory precursors from a common territory: cell sorting and reciprocity of Dlx5 and Pax6 expression. *Dev. Biol.* **271**, 403-414.

Bovolenta, P. and Dodd, J. (1991). Perturbation of neuronal differentiation and axon guidance in the spinal cord of mouse embryos lacking a floor plate: analysis of Danforth's short-tail mutation. *Development* **113**, 625-639.

Breau, M. A. and Schneider-Maunoury, S. (2014). Mechanisms of cranial placode assembly. *Int. J. Dev. Biol.* **58**, 9-19.

Breau, M. A. and Schneider-Maunoury, S. (2015). Cranial placodes: models for exploring the multi-facets of cell adhesion in epithelial rearrangement, collective migration and neuronal movements. *Dev. Biol.* **401**, 25-36.

Cajal, M., Lawson, K. A., Hill, B., Moreau, A., Rao, J., Ross, A., Collignon, J. and Camus, A. (2012). Clonal and molecular analysis of the prospective anterior neural boundary in the mouse embryo. *Development* **139**, 423-436.

Cajal, M., Creuzet, S. E., Papanayotou, C., Saberan-Djoneidi, D., Chuva de Sousa Lopes, S. M., Zwijsen, A., Collignon, J. and Camus, A. (2014). A conserved role for non-neural ectoderm cells in early neural development. *Development* **141**, 4127-4138.

Camus, A., Davidson, B. P., Billiards, S., Khoo, P., Rivera-Perez, J. A., Wakamiya, M., Behringer, R. R. and Tam, P. P. (2000). The morphogenetic role of midline mesendoderm and ectoderm in the development of the forebrain and the midbrain of the mouse embryo. *Development* **127**, 1799-1813.

Chiang, C., Litingtung, Y., Lee, E., Young, K. E., Corden, J. L., Westphal, H. and Beachy, P. A. (1996). Cyclopia and defective axial patterning in mice lacking Sonic hedgehog gene function. *Nature* **383**, 407-413.

Chizhikov, V. V., Lindgren, A. G., Mishima, Y., Roberts, R. W., Aldinger, K. A., Miesegaes, G. R., Currle, D. S., Monuki, E. S. and Millen, K. J. (2010). Lmx1a regulates fates and location of cells originating from the cerebellar rhombic lip and telencephalic cortical hem. *Proc. Natl. Acad. Sci. USA* **107**, 10725-10730.

Chou, S.-J., Hermesz, E., Hatta, T., Feltner, D., El-Hodiri, H. M., Jamrich, M. and Mahon, K. (2006). Conserved regulatory elements establish the dynamic expression of Rpx/HesxI in early vertebrate development. *Dev. Biol.* **292**, 533-545.

Cobos, I., Shimamura, K., Rubenstein, J. L. R., Martínez, S. and Puelles, L. (2001). Fate map of the avian anterior forebrain at the four-somite stage, based on the analysis of quail-chick chimeras. *Dev. Biol.* **239**, 46-67.

Costello, I., Nowotschin, S., Sun, X., Mould, A. W., Hadjantonakis, A.-K., Bikoff, E. K. and Robertson, E. J. (2015). Lhx1 functions together with Otx2, Foxa2, and Ldb1 to govern anterior mesendoderm, node, and midline development. *Genes Dev.* **29**, 2108-2122.

Couly, G. and Le Douarin, N. M. (1988). The fate map of the cephalic neural primordium at the presomitic to the 3-somite stage in the avian embryo. *Development* **103** Suppl., 101-113.

Dattani, M. T., Martinez-Barbera, J.-P., Thomas, P. Q., Brickman, J. M., Gupta, R., Mårtensson, I.-L., Toresson, H., Fox, M., Wales, J. K. H., Hindmarsh, P. C. et al. (1998). Mutations in the homeobox gene HESX1/Hesx1 associated with septo-optic dysplasia in human and mouse. *Nat. Genet.* **19**, 125-133.

Devine, C. A., Sbrogna, J. L., Guner, B., Osgood, M., Shen, M.-C. and Karlstrom, R. O. (2009). A dynamic Gli code interprets Hh signals to regulate induction, patterning, and endocrine cell specification in the zebrafish pituitary. *Dev. Biol.* **326**, 143-154.

Dutta, S., Dietrich, J. E., Aspock, G., Burdine, R. D., Schier, A., Westerfield, M. and Varga, Z. M. (2005). pitx3 defines an equivalence domain for lens and anterior pituitary placode. *Development* **132**, 1579-1590.

Eagleson, G., Ferreiro, B. and Harris, W. A. (1995). Fate of the anterior neural ridge and the morphogenesis of the Xenopus forebrain. *J. Neurobiol.* **28**, 146-158.

ElAmraoui, A. and Dubois, P. M. (1993). Experimental evidence for the early commitment of the presumptive adenohypophysis. *Neuroendocrinology* **58**, 609-615.

Esteve, P. and Bovolenta, P. (1999). cSix4, a member of the six gene family of transcription factors, is expressed during placode and somite development. *Mech. Dev.* **85**, 161-165.

Firmino, J., Rocancourt, D., Saadaoui, M., Moreau, C. and Gros, J. (2016). Cell division drives epithelial cell rearrangements during gastrulation in chick. *Dev. Cell* **36**, 249-261.

Gallardo, M. E., Lopez-Rios, J., Fernaud-Espinosa, I., Granadino, B., Sanz, R., Ramos, C., Ayuso, C., Seller, M. J., Brunner, H. G., Bovolenta, P. et al. (1999). Genomic cloning and characterization of the human homeobox gene SIX6 reveals a cluster of SIX genes in chromosome 14 and associates SIX6 hemizygosity with bilateral anophthalmia and pituitary anomalies. *Genomics* **61**, 82-91.

Graham, A. and Shimeld, S. M. (2013). The origin and evolution of the ectodermal placodes. *J. Anat.* **222**, 32-40.

Guner, B., Ozacar, A. T., Thomas, J. E. and Karlstrom, R. O. (2008). Graded hedgehog and fibroblast growth factor signaling independently regulate pituitary cell fates and help establish the pars distalis and pars intermedia of the zebrafish adenohypophysis. *Endocrinology* **149**, 4435-4451.
Hamburger, V. and Hamilton, H. L. (1951). A series of normal stages in the development of the chick embryo. *Dev. Dyn.* **195**, 231-272.
Hatta, K., Kimmel, C. B., Ho, R. K. and Walker, C. (1991). The cyclops mutation blocks specification of the floor plate of the zebrafish central nervous system. *Nature* **350**, 339-341.
Herzog, W., Zeng, X., Lele, Z., Sonntag, C., Ting, J.-W., Chang, C.-Y. and Hammerschmidt, M. (2003). Adenohypophysis formation in the zebrafish and its dependence on sonic hedgehog. *Dev. Biol.* **254**, 36-49.
Herzog, W., Sonntag, C., von der, H. S., Roehl, H. H., Varga, Z. M. and Hammerschmidt, M. (2004). Fgf3 signaling from the ventral diencephalon is required for early specification and subsequent survival of the zebrafish adenohypophysis. *Development* **131**, 3681-3692.
Kasberg, A. D., Brunskill, E. W. and Steven Potter, S. (2013). SP8 regulates signaling centers during craniofacial development. *Dev. Biol.* **381**, 312-323.
Klar, A., Baldassare, M. and Jessell, T. M. (1992). F-spondin: a gene expressed at high levels in the floor plate encodes a secreted protein that promotes neural cell adhesion and neurite extension. *Cell* **69**, 95-110.
Kobayashi, M., Osanai, H., Kawakami, K. and Yamamoto, M. (2000). Expression of three zebrafish Six4 genes in the cranial sensory placodes and the developing somites. *Mech. Dev.* **98**, 151-155.
Kondoh, H., Uchikawa, M., Yoda, H., Takeda, H., Furutani-Seiki, M. and Karlstrom, R. O. (2000). Zebrafish mutations in Gli-mediated hedgehog signaling lead to lens transdifferentiation from the adenohypophysis anlage. *Mech. Dev.* **96**, 165-174.
Kozlowski, D. J., Murakami, T., Ho, R. K. and Weinberg, E. S. (1997). Regional cell movement and tissue patterning in the zebrafish embryo revealed by fate mapping with caged fluorescein. *Biochem. Cell Biol.* **75**, 551-562.
Kwon, H.-J., Bhat, N., Sweet, E. M., Cornell, R. A. and Riley, B. B. (2010). Identification of early requirements for preplacodal ectoderm and sensory organ development. *PLoS Genet.* **6**, e1001133.
Li, X., Perissi, V., Liu, F., Rose, D. W. and Rosenfeld, M. G. (2002). Tissue-specific regulation of retinal and pituitary precursor cell proliferation. *Science* **297**, 1180-1183.
Litsiou, A., Hanson, S. and Streit, A. (2005). A balance of FGF, BMP and WNT signalling positions the future placode territory in the head. *Development* **132**, 4051-4062.
Lleras-Forero, L., Tambalo, M., Christophorou, N., Chambers, D., Houart, C. and Streit, A. (2013). Neuropeptides: developmental signals in placode progenitor formation. *Dev. Cell* **26**, 195-203.
López-Ríos, J., Gallardo, M. E., Rodriguez de Córdoba, S. and Bovolenta, P. (1999). Six9 (Optx2), a new member of the six gene family of transcription factors, is expressed at early stages of vertebrate ocular and pituitary development. *Mech. Dev.* **83**, 155-159.
Maden, M., Blentic, A., Reijntjes, S., Seguin, S., Gale, E. and Graham, A. (2007). Retinoic acid is required for specification of the ventral eye field and for Rathke's pouch in the avian embryo. *Int. J. Dev. Biol.* **51**, 191-200.
McCabe, K. L. and Bronner-Fraser, M. (2009). Molecular and tissue interactions governing induction of cranial ectodermal placodes. *Dev. Biol.* **332**, 189-195.
Mendes, R. V., Martins, G. G., Cristovão, A. M. and Saúde, L. (2014). N-cadherin locks left-right asymmetry by ending the leftward movement of Hensen's node cells. *Dev. Cell* **30**, 353-360.
Mishima, Y., Lindgren, A. G., Chizhikov, V. V., Johnson, R. L. and Millen, K. J. (2009). Overlapping function of Lmx1a and Lmx1b in anterior hindbrain roof plate formation and cerebellar growth. *J. Neurosci.* **29**, 11377-11384.
Moody, S. A. and LaMantia, A.-S. (2015). Transcriptional regulation of cranial sensory placode development. *Curr. Top. Dev. Biol.* **111**, 301-350.
Parkinson, N., Collins, M. M., Dufresne, L. and Ryan, A. K. (2010). Expression patterns of hormones, signaling molecules, and transcription factors during adenohypophysis development in the chick embryo. *Dev. Dyn.* **239**, 1197-1210.
Pieper, M., Eagleson, G. W., Wosniok, W. and Schlosser, G. (2011). Origin and segregation of cranial placodes in Xenopus laevis. *Dev. Biol.* **360**, 257-275.
Price, S. R., De Marco Garcia, N. V., Ranscht, B. and Jessell, T. M. (2002). Regulation of motor neuron pool sorting by differential expression of type II cadherins. *Cell* **109**, 205-216.
Prince, K. L., Walvoord, E. C. and Rhodes, S. J. (2011). The role of homeodomain transcription factors in heritable pituitary disease. *Nat. Rev. Endocrinol.* **7**, 727-737.
Ruiz i Altaba, A. and Jessell, T. M. (1993). Midline cells and the organization of the vertebrate neuraxis. *Curr. Opin. Genet. Dev.* **3**, 633-640.
Saint-Jeannet, J.-P. and Moody, S. A. (2014). Establishing the pre-placodal region and breaking it into placodes with distinct identities. *Dev. Biol.* **389**, 13-27.
Sajedi, E., Gaston-Massuet, C., Signore, M., Andoniadou, C. L., Kelberman, D., Castro, S., Etchevers, H. C., Gerrelli, D., Dattani, M. T. and Martinez-Barbera, J. P. (2008). Analysis of mouse models carrying the I26T and R160C substitutions in the transcriptional repressor HESX1 as models for septo-optic dysplasia and hypopituitarism. *Dis. Model Mech.* **1**, 241-254.
Sanchez-Arrones, L., Stern, C. D., Bovolenta, P. and Puelles, L. (2012). Sharpening of the anterior neural border in the chick by rostral endoderm signalling. *Development* **139**, 1034-1044.
Sánchez-Arrones, L., Ferrán, J. L., Hidalgo-Sanchez, M. and Puelles, L. (2015). Origin and early development of the chicken adenohypophysis. *Front. Neuroanat.* **9**, 7.
Sato, S., Ikeda, K., Shioi, G., Ochi, H., Ogino, H., Yajima, H. and Kawakami, K. (2010). Conserved expression of mouse Six1 in the pre-placodal region (PPR) and identification of an enhancer for the rostral PPR. *Dev. Biol.* **344**, 158-171.
Sbrogna, J. L., Barresi, M. J. F. and Karlstrom, R. O. (2003). Multiple roles for Hedgehog signaling in zebrafish pituitary development. *Dev. Biol.* **254**, 19-35.
Schlosser, G. (2006). Induction and specification of cranial placodes. *Dev. Biol.* **294**, 303-351.
Schlosser, G. (2014). Early embryonic specification of vertebrate cranial placodes. *Wiley Interdiscip. Rev. Dev. Biol.* **3**, 349-363.
Schlosser, G. and Ahrens, K. (2004). Molecular anatomy of placode development in Xenopus laevis. *Dev. Biol.* **271**, 439-466.
Seth, A., Machingo, Q. J., Fritz, A. and Shur, B. D. (2010). Core fucosylation is required for midline patterning during zebrafish development. *Dev. Dyn.* **239**, 3380-3390.
Shawlot, W. and Behringer, R. R. (1995). Requirement for Lim1 in head-organizer function. *Nature* **374**, 425-430.
Shawlot, W., Wakamiya, M., Kwan, K. M., Kania, A., Jessell, T. M. and Behringer, R. R. (1999). Lim1 is required in both primitive streak-derived tissues and visceral endoderm for head formation in the mouse. *Development* **126**, 4925-4932.
Sheng, H. Z., Zhadanov, A. B., Mosinger, B., Jr, Fujii, T., Bertuzzi, S., Grinberg, A., Lee, E. J., Huang, S.-P., Mahon, K. A. and Westphal, H. (1996). Specification of pituitary cell lineages by the LIM homeobox gene Lhx3. *Science* **272**, 1004-1007.
Sjödal, M. and Gunhaga, L. (2008). Expression patterns of Shh, Ptc2, Raldh3, Pitx2, Isl1, Lim3 and Pax6 in the developing chick hypophyseal placode and Rathke's pouch. *Gene Expr. Patterns* **8**, 481-485.
Stern, C. D. and Bachvarova, R. (1997). Early chick embryos in vitro. *Int. J. Dev. Biol.* **41**, 379-387.
Steventon, B., Mayor, R. and Streit, A. (2016). Directional cell movements downstream of Gbx2 and Otx2 control the assembly of sensory placodes. *Biol. Open* **5**, 1620-1624.
Streit, A. (2002). Extensive cell movements accompany formation of the otic placode. *Dev. Biol.* **249**, 237-254.
Streit, A. (2004). Early development of the cranial sensory nervous system: from a common field to individual placodes. *Dev. Biol.* **276**, 1-15.
Streit, A. (2007). The preplacodal region: an ectodermal domain with multipotential progenitors that contribute to sense organs and cranial sensory ganglia. *Int. J. Dev. Biol.* **51**, 447-461.
Toro, S. and Varga, Z. M. (2007). Equivalent progenitor cells in the zebrafish anterior preplacodal field give rise to adenohypophysis, lens, and olfactory placodes. *Semin. Cell Dev. Biol.* **18**, 534-542.
Trousse, F., Esteve, P. and Bovolenta, P. (2001). Bmp4 mediates apoptotic cell death in the developing chick eye. *J. Neurosci.* **21**, 1292-1301.
Uchida, K., Murakami, Y., Kuraku, S., Hirano, S. and Kuratani, S. (2003). Development of the adenohypophysis in the lamprey: evolution of epigenetic patterning programs in organogenesis. *J. Exp. Zool. B. Mol. Dev. Evol.* **300**, 32-47.
van Straaten, H. W., Hekking, J. W. M., Wiertz-Hoessels, E. J. L. M., Thors, F. and Drukker, J. (1988). Effect of the notochord on the differentiation of a floor plate area in the neural tube of the chick embryo. *Anat. Embryol.* **177**, 317-324.
Voiculescu, O., Papanayotou, C. and Stern, C. D. (2008). Spatially and temporally controlled electroporation of early chick embryos. *Nat. Protoc.* **3**, 419-426.
Whitlock, K. E. and Westerfield, M. (2000). The olfactory placodes of the zebrafish form by convergence of cellular fields at the edge of the neural plate. *Development* **127**, 3645-3653.
Xu, H., Dude, C. M. and Baker, C. V. H. (2008). Fine-grained fate maps for the ophthalmic and maxillomandibular trigeminal placodes in the chick embryo. *Dev. Biol.* **317**, 174-186.
Zhao, Y., Morales, D. C., Hermesz, E., Lee, W.-K., Pfaff, S. L. and Westphal, H. (2006). Reduced expression of the LIM-homeobox gene Lhx3 impairs growth and differentiation of Rathke's pouch and increases cell apoptosis during mouse pituitary development. *Mech. Dev.* **123**, 605-613.

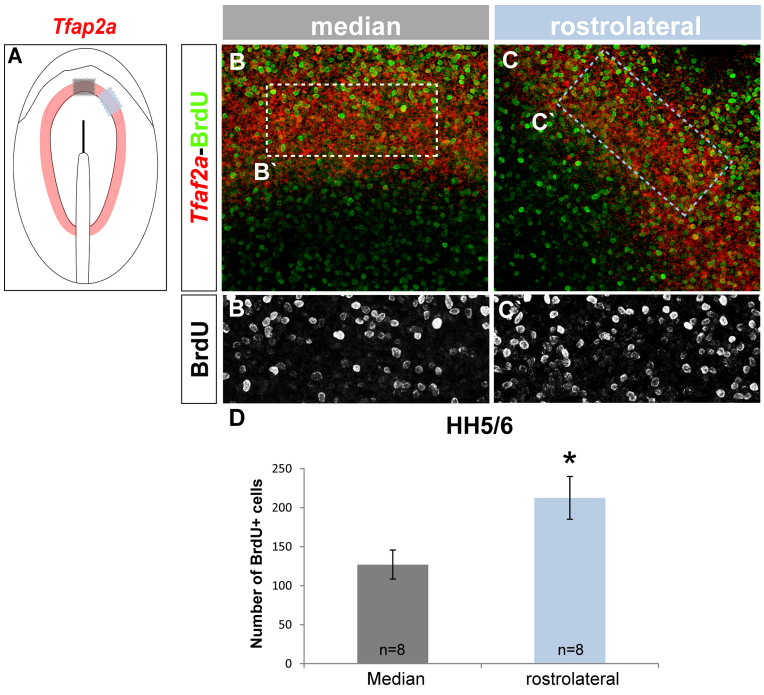

Figure S1

Figure S1. Median and rostrolateral PPE cells present different mitotic rates. A) Schematic representation of a HH5/6 embryo with the PPE in pink and the analysed median and rostrolateral PPE areas are represented as grey and blue boxes. B-C') Confocal dorsal views of embryos hybridized *in toto* with a probe for the placodal marker *Tfap2a* and immunostained for BrdU. B' and C' are a high magnification views in B, C. D) Quantification of the number of BrdU positive cells in median (n embryos =8) and rostrolateral (n=8) PPE at HH5/6 (* $p < 0.05$, Student's *t*-test; error bars indicate mean ± s.e.m.).

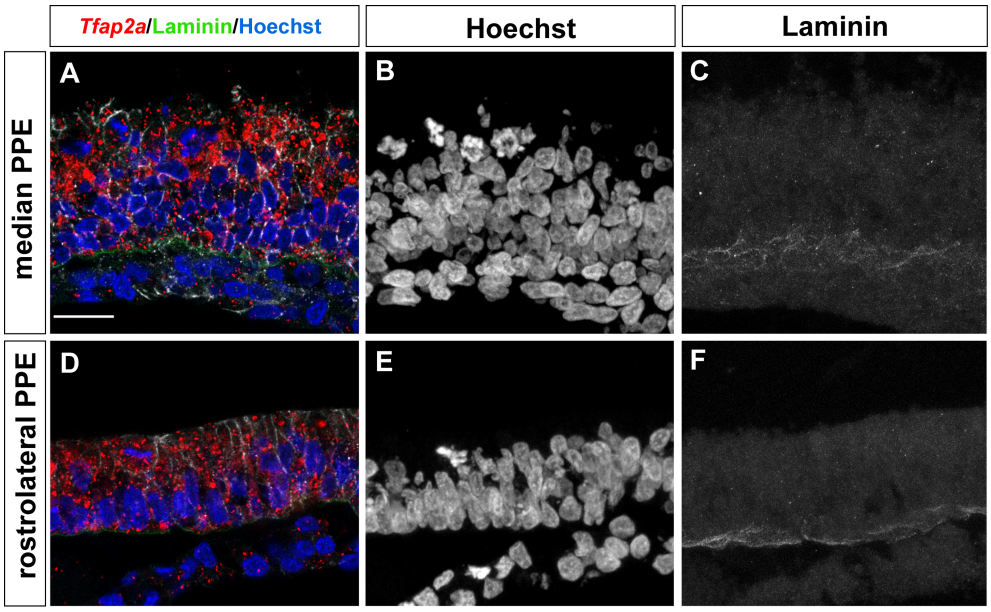

Figure S2

Figure S2. The median PPE is superimposed to the mesendoderm. Frontal sections of HH6/7 embryos (n=6) hybridized *in toto* with a probe for *Tfap2a* and immunostained with antibodies against laminin (A,D). Note the absence of signal underneath the AHP prospective region (A-C). Immunostaining is instead prominent at the level of the rostrolateral PPE (D-F). Scale bar: 20 µm.

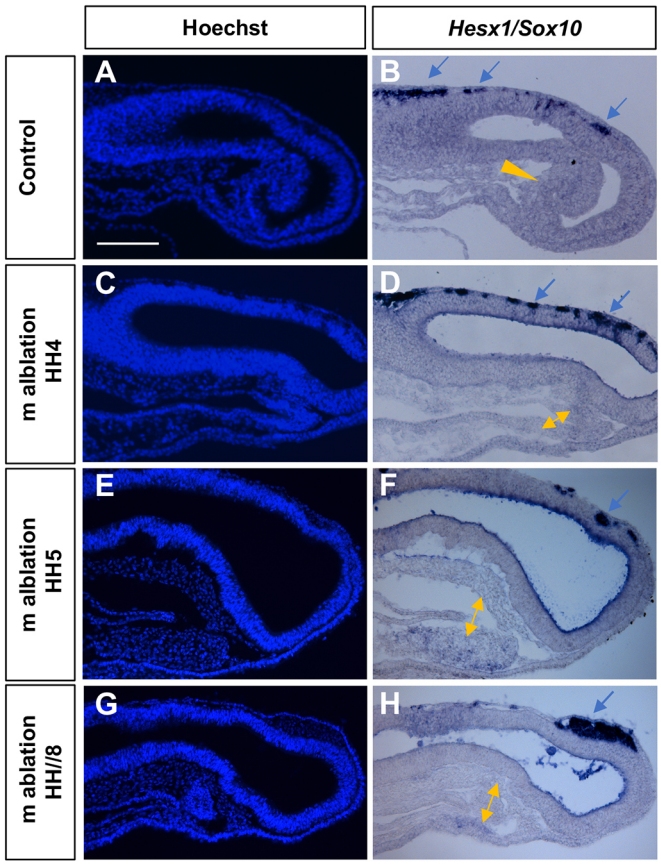

Supplementary Figure 3

Figure S3. Ablations of the median PPE leaves the underlying mesendoderm intact. Sagittal sections of HH10/11 embryos with (C-H) or without (A, B) median PPE ablations performed at the stages indicated in the panels. Embryos were hybridized with probes specific for *Sox10* and *Hesx1* to detect the presence of the neural crest and mesendoderm, respectively. Blue arrows indicate *Sox10* positive neural crest cells, double yellow arrows point to the *Hesx1*-positive mesendoderm. Note that ablation of the median PPE does not affect these tissues. Scale bar:50 µm.

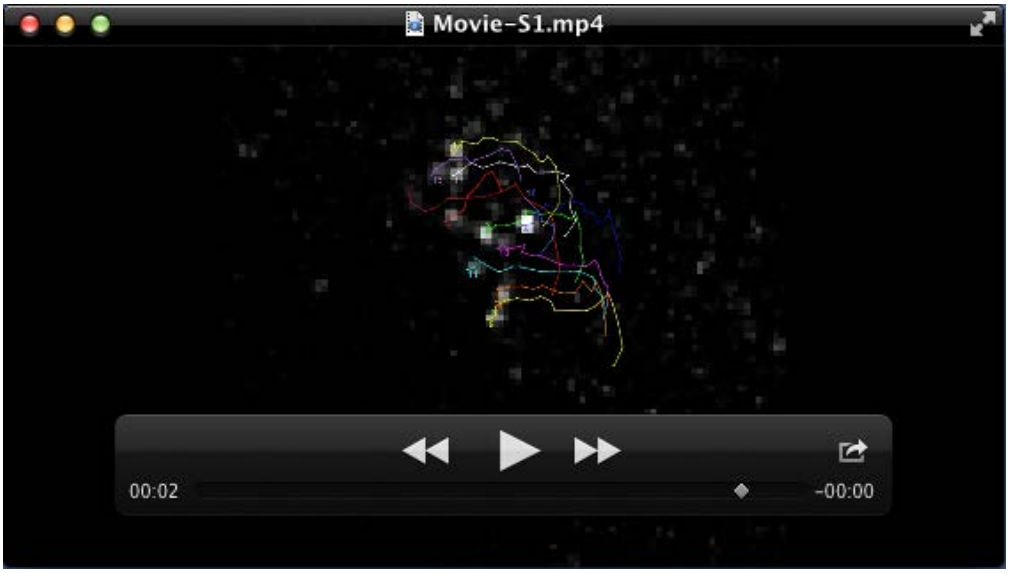

Movie 1: Cells in the rostolateral PPE undergo medio-lateral intercalating movements. The movie shows an example of an embryo in which a plasmid carrying the photo-convertible *Kaede* sequence was electroporated at gastrula stage in the rostrolateral PPE domain. After four hours, few kaede-expressing cells positioned in the rostrolateral PPE were hit with a laser beam to photoconvert the kaede to red. The behaviour of red-labelled cells was recorded for the next few hours until the embryo reached stage HH5+/6. Note the medio-lateral movements of the cells.

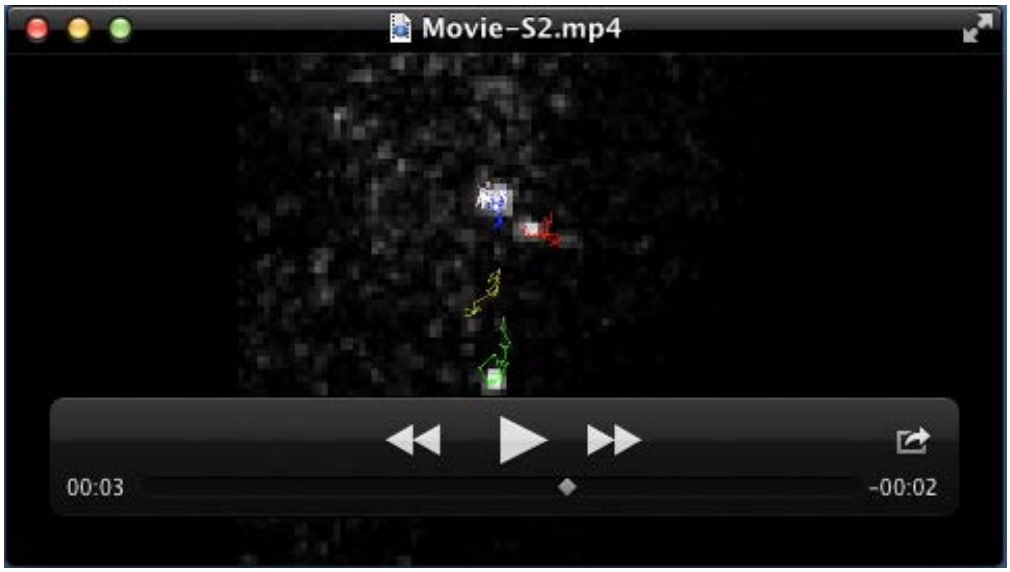

Movie 2: Cells in the medial PPE hardly move from their position. The movie shows an example of an embryo in which a plasmid carrying the photo-convertible *Kaede* sequence was electroporated at gastrula stage in the median PPE domain. After four hours, few kaede-expressing cells positioned in the median PPE were hit with a laser beam to photoconvert the kaede to red. The behaviour of red-labelled cells was recorded for the next few hours until the embryo reached stage HH8/9.

Table S1. List of the labelling experiments performed to obtain the fate map of adenohypophysis placode precursors. The table reports the parameters used to position the initial and final position of the labelled cells for each one of the performed experiment (case). The final position of labelled cells is color coded: adenohypophysis placode (red), adenohypophysis and olfactory (yellow), olfactory only (light green); olfactory and lens (bright green); lens only (blue).

Click here to Download Table S1

Table S2. List of the genes enriched in either the medial or rostrolateral placodal explants. The table shows all the genes found enriched in either the medial or the rostro-lateral placodes expressed in Log2 (fold change) and the related p and q values and proposed function of the genes

Click here to Download Table S2